Applied Physics A (2024) 130:367
https://doi.org/10.1007/s00339-024-07511-w

Applied Physics A
Materials Science & Processing

Light-triggered defect dynamics in silicon wafers: understanding degradation mechanisms

Yougherta Chibane[1] · Yacine Kouhlane[2] · Djoudi Bouhafs[3] · Wafa Achour[3] · Asmaa Mohammed-Krarroubi[3] · Amar Khelfane[3]

Received: 3 February 2024 / Accepted: 5 April 2024 / Published online: 3 May 2024

Abstract
In this work, the effect of heat treatment on the minority carrier lifetime (τ) in boron-doped crystalline silicon wafers coated with a silicon nitride (SiNx:H) layer has been investigated. The results showed an initial increase in τ during the early phase of light exposure of the samples, which was attributed to the presence of iron–boron complexes in the c-Si wafers. However, this enhancement was followed by a decrease associated with the formation of boron-oxygen complexes, known as light-induced degradation. Moreover, kinetic models were used to analyze defect interactions in the wafers, showing a correlation between τ behavior and hydrogen-boron complex concentrations, and related by analytical techniques. In addition, the samples were subjected to a dark annealing step, resulting in further degradation due to the firing temperature process and the presence of hydrogen atoms in the silicon nitride layer. Finally, this study provides valuable insights into defect formation mechanisms in c-Si wafers that could improve the stability and efficiency optimization of silicon-based solar cells under operating conditions.

Keywords LID · RTP process · Silicon wafer · SiNx:H layer · Minority carrier lifetime

1 Introduction

There are several aspects that make Silicon the main material used in solar cell production: abundance, cost, and rapid innovation [1–9]. Silicon wafer-based solar cells currently represent approximately 95% of photovoltaic production [7]. According to the International Technology Roadmap for Photovoltaics [6], p-type boron-doped silicon wafers grown by the Czochralski method (Cz-Si) still hold a significant share of the market in 2023 and will remain one of the dominant materials over the next decade. Crystalline silicon solar cells are widely used worldwide as stable photovoltaic devices. Since becoming a clean energy source, researchers have been actively working to improve their efficiency to make them an interesting alternative to conventional energy sources [10]. Photovoltaic solar systems have experienced a stunning cost reduction due to a significant decrease in manufacturing costs and higher efficiency of devices [4, 11–13]. The silicon wafer substrate represents a substantial fraction of the total cost, and the quality of its material is one of the key factors determining the overall efficiency of the device [14]. However, silicon-based solar cell exposed to illumination are susceptible to a drop in performance. This drop occurs due to various bulk degradation mechanisms [14–16] and surface-related mechanisms [17, 18], which are typically accelerated by temperature and carrier injection [19]. These degradation modes can lead to serious power losses and thus pose a challenge for silicon solar cell manufacturers. Over the past decades, research has focused on mass-related degradation [20]. Both universities and industry have paid considerable attention to both light-induced degradation (LID) [21–23] and light and elevated temperature-induced degradation (LeTID) [24, 25]. For boron-doped silicon solar cells, light-induced degradation has gained relevance [5, 12, 15, 26–28].

✉ Yougherta Chibane
chibaneyougherta@gmail.com

[1] Laboratory of Semiconductors (LSC), Department of Physics, Faculty of Sciences, Badji Mokhtar University, Annaba, Algeria

[2] Laboratory of Advanced Systems and Materials (LASMA), Department of Physics, Faculty of Sciences, Badji Mokhtar University, Annaba, Algeria

[3] Research Center in Semiconductor Technology for the Energetic (CRTSE), Algiers, Algeria

The LID effect is closely related to the charge carrier's lifetime behavior in the silicon material, when sunlight interacts with the solar cell, it sets off a complex interaction of defects formation [27, 29, 30] that affect the charge carrier dynamics, and consequently, they affect the conversion efficiency in the solar cell [31]. In this optics, we investigate the impact of LID on p-type silicon wafers that undergo a fast-firing step in a rapid thermal processing (RTP) oven. Unlike previous research, which often generalized degradation effects, our approach systematically investigates the charge carrier lifetime (τ) under various test conditions using the quasi-steady-state photoconductance (QSSPC) method. Moreover, by integrating analytical techniques such as Fourier transform infrared (FTIR) and photoluminescence (PL) spectroscopy, we aim to better understand the correlation between defect formation and the thermal history of the materials, with a special emphasis on passivation layers. Further, the interdisciplinary approach includes experimental investigations and simulation based on kinetic models to validate existing theories and assess the role of the firing step in defect formation. In addition, the discussion on the potential interaction between hydrogen (H) species and dopant atoms adds a new dimension to the understanding of electrical kinetics changes triggered by light-induced degradation. Through this comprehensive approach, the study not only seeks to deepen the knowledge of LID mechanisms but also provide predictive insights for mitigation strategies.

2 Experimental

In this work, we use a commercially available boron-doped silicon wafers from Siltronix grown by the Czochralski (Cz) method of 360 µm thickness, with a doping concentration of $N_{dop} = 10^{16}$ cm^{-3} and a resistivity ρ equal to 2.7 Ω/cm. Prior to the investigation, the wafers underwent typical preparation involving chemical etching followed by deoxidation, resulting in a clean surface for subsequent processing. Next, a set of samples were coated at 380 °C with an 80 nm thickness, silicon nitride (SiNx:H) layer using a plasma-enhanced chemical vapor deposition (PECVD) tool. Moreover, to investigate the impact of firing on minority carrier lifetime (τ), a subset of wafers received rapid thermal annealing (RTA) treatment at varying peak temperatures (680, 730, 750, and 800 °C) using AccuThermo610 AW rapid thermal processing (RTP) furnace. Additionally, another set was subjected to a dedicated gettering protocol [14–32]. The wafers are diffused in a furnace tube with $POCl_3$ flow at around 800–900 °C, leading to efficient gettering of transition metal impurities, while a final group served as untreated references. Fourier transform infrared (FTIR) and photoluminescence (PL) spectroscopy were employed on all passivated samples to control the quality of the simples after heat treatment. Carrier lifetime measurements were systematically performed at each processing stage using the quasi-steady-state photoconductance (QSSPC) technique (Sinton Instruments WCT-120) [33]. Finally, the design of experimental processes is shown in Fig. 1.

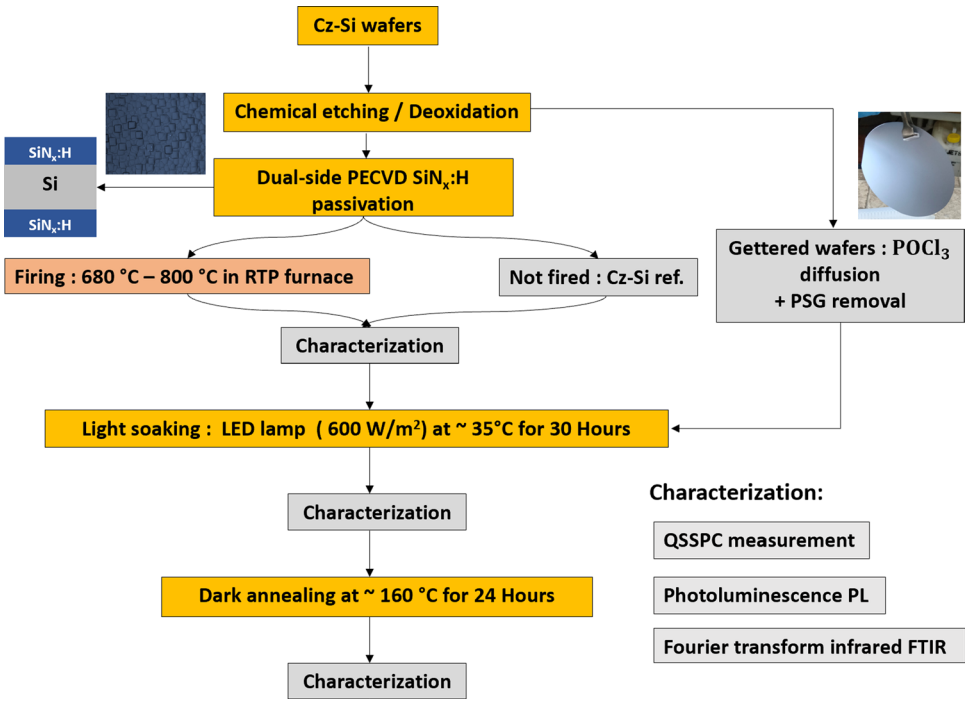

Fig. 1 Process flow diagram

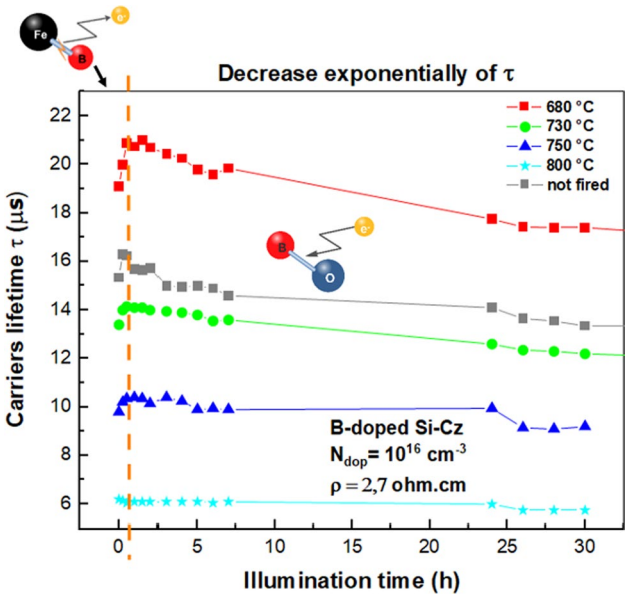

Fig. 2 Minority carrier lifetime (τ) of fired (from 680 to 800 °C) and unfired simples as functions of illumination time

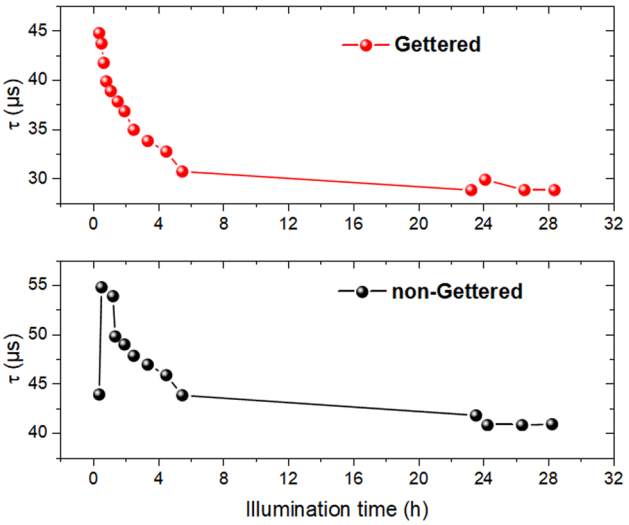

Fig. 3 Lifetime curves for gettered and non-gettered wafers as functions of illumination time

3 Results and discussions

3.1 Light induced degradation LID (light soaking)

Figure 2 depicts the time evolution of minority carrier lifetime (τ) in samples with passivation layer and treated at different RTP peaks temperatures. Moreover, τ exhibits a pronounced exponential decay with increasing illumination time [5, 15, 26, 27, 34]. This initial rise in τ observed within the first hour of illumination can be attributed to the activity of iron–boron (Fe–B) complex [35–38]. The dissociation of these complexes effectively eliminates their related recombination centers, consequently enhancing the minority carrier lifetime [39–41]. Further, the highest carrier lifetime values occur at about 680 °C (Fig. 2). This phenomenon can be attributed to the intricate interplay of hydrogen diffusion and passivation produced by the SiNx:H layer onto the silicon substrate [42]. However, increasing the temperature reduces the carrier's lifetime, implying a possible defect formation within the SiNx:H layer due to the RTP process [43]. Furthermore, temperatures exceeding 680 °C lead to a significant decline in carrier lifetime, indicating severe damage to the SiNx:H layer likely caused by formation of cracks [44]. The results suggest that Rapid Thermal Processing (RTP) is most effective at around 680 °C for maximizing carrier's lifetime for samples passivated with SiNx:H layers which is consistent with existing literature [45].

The evolution of minority carrier lifetime (τ) with illumination time for both gettered and non-gettered samples is illustrated in Fig. 3. Also, non-gettered wafers exhibit a distinct initial increase in τ within the first stages of light exposure, followed by a subsequent exponential decay. This initial rise of τ can be attributed to the dissociation of Fe–B pairs. It is known that dissociations of Fe–B pairs in a silicon-based semiconductor are accompanied by a change in the minority carrier lifetime [41]. The Fe–B complexes are well-documented defects in crystalline silicon (c-Si) wafers arising from the bonding of iron and boron impurities [36, 46–48]. These complexes act as recombination centers. The regeneration processes activated by light exposure dissociate these Fe–B pairs, eliminating their recombination activity and consequently increasing τ.

On the other hand, wafers subjected to a gettered treatment to reduce iron concentration, exhibit a significantly lower density of Fe–B pairs compared to their non-gettered samples [4, 14, 32]. The Fe–B complex dissociation effect in the illumination process is absent in the initial τ for the gettered samples, as evident in Fig. 3. In general, metals act as powerful recombination centers in silicon wafers, thus degrading the efficiency of solar cells. By relocating metals to a region of the device where they have less impact on the overall device performance, the getter improves cell efficiency as a result [4].

3.2 Optical characterization for Cz-Si wafers

Figure 4 shows the Fourier transform infrared (FTIR) spectra results of the silicon wafers with SiNx:H layers following RTP process at different temperatures. The gray curve corresponds to the non-treated reference sample. The progressive decrease in the intensity of absorption peaks such as: silicon–nitride (Si–N), silicon–silicon (Si–Si),

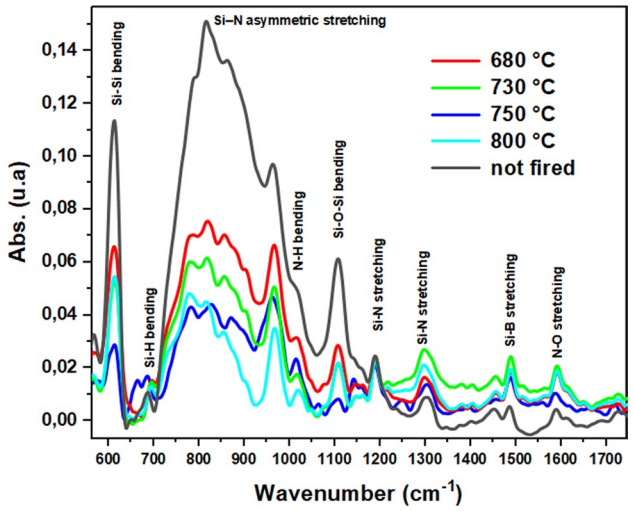

Fig. 4 FTIR spectra results of SiNx:H films deposited on c-Si substrates and post-annealed at different temperatures in an RTP furnace

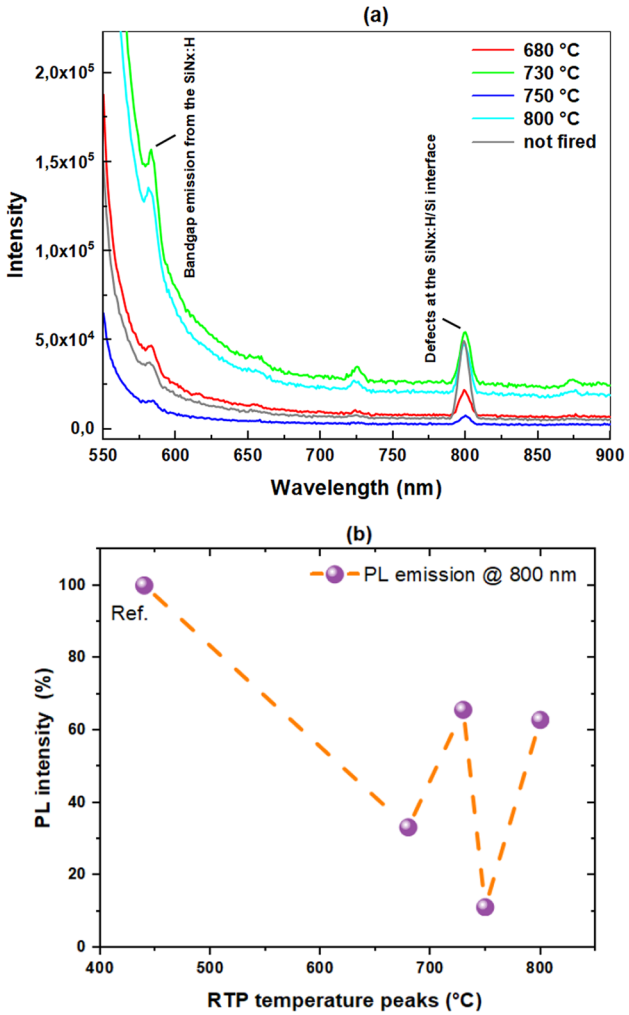

Fig. 5 The obtained results of: **a** PL spectra under excitation of 532 nm of a SiNx:H films deposited on c-Si substrates and **b** PL intensity emission comparison at 800 °C for treated and non-treated samples (**b**)

silicon–oxygen–silicon (Si–O–Si) and nitride–hydrogen (N–H) bonds compared to the reference sample spectrum with increasing annealing temperature, is clearly observed in Fig. 4. This trend indicates a reduced strength of these bonds altered by the annealing process [45], implying a degradation of the atomic structure within the SiNx:H layers [49, 50]. In extreme cases, under sufficiently high temperatures, the annealing process can even induce the formation of crystalline bonds within the amorphous SiNx:H layer [51].

Photoluminescence (PL) spectra of the samples are shown in Fig. 5. The excitation wavelength for all the samples is 532 nm. The peak at 583 nm (2.13 eV) is related to the defect energy levels within the gap of nanometer-size amorphous silicon nitride layers [52, 53]. Moreover, an emission in the infrared region at peak of 800 nm (1.55 eV), clearly demonstrates a silicon/SiNx:H interface luminescence [53, 54]. We presumed that by RTP treatment at high temperatures, some atomic bonds are broken and reconfigured from silicon/ SiNx:H interface.

3.3 Comparison of lifetime curves for samples under light and dark annealing conditions

Comparison of evolution of τ curves for the treated samples under light soaking (LS) and dark annealing (DA) conditions are given in Fig. 6. Moreover, the lifetime generated in the dark annealing test is typically greater than that generated in LS test. In addition, the difference in values between the two tests increases with the annealing temperature. The rate variation over time for both the LS and DA tests exhibit a similar pattern during the initial phase (approximately 0–5 h), as reported in the literature [55]. However, after this initial phase, the lifetime under DA shifts from regeneration for the reference sample to gradual degradation, depending on the peak RTP temperature. Lin et al. [22] recently showed that the rate constants τ_{reg} and τ_{deg} depend on the maximum annealing temperature. Kersten et al. [55] observed that SiNx:H passivated and fired samples showed degradation after 1000 h of DA at 75 °C. The experimental results (Fig. 2) show that peak firing temperatures resulted in higher deterioration of τ, and this effect cannot be attributed to iron– boron pairs or even boron–oxygen defects. Recently, it has been widely reported that hydrogen is responsible for the formation and activation of certain defects in crystalline silicon [22, 56, 57]. In their work, Lin et al. [22] and Ciesla et al. [58] demonstrate that high levels of hydrogen may initiate defects independently. The behavior of hydrogen in boron-doped silicon has been studied in several recent studies

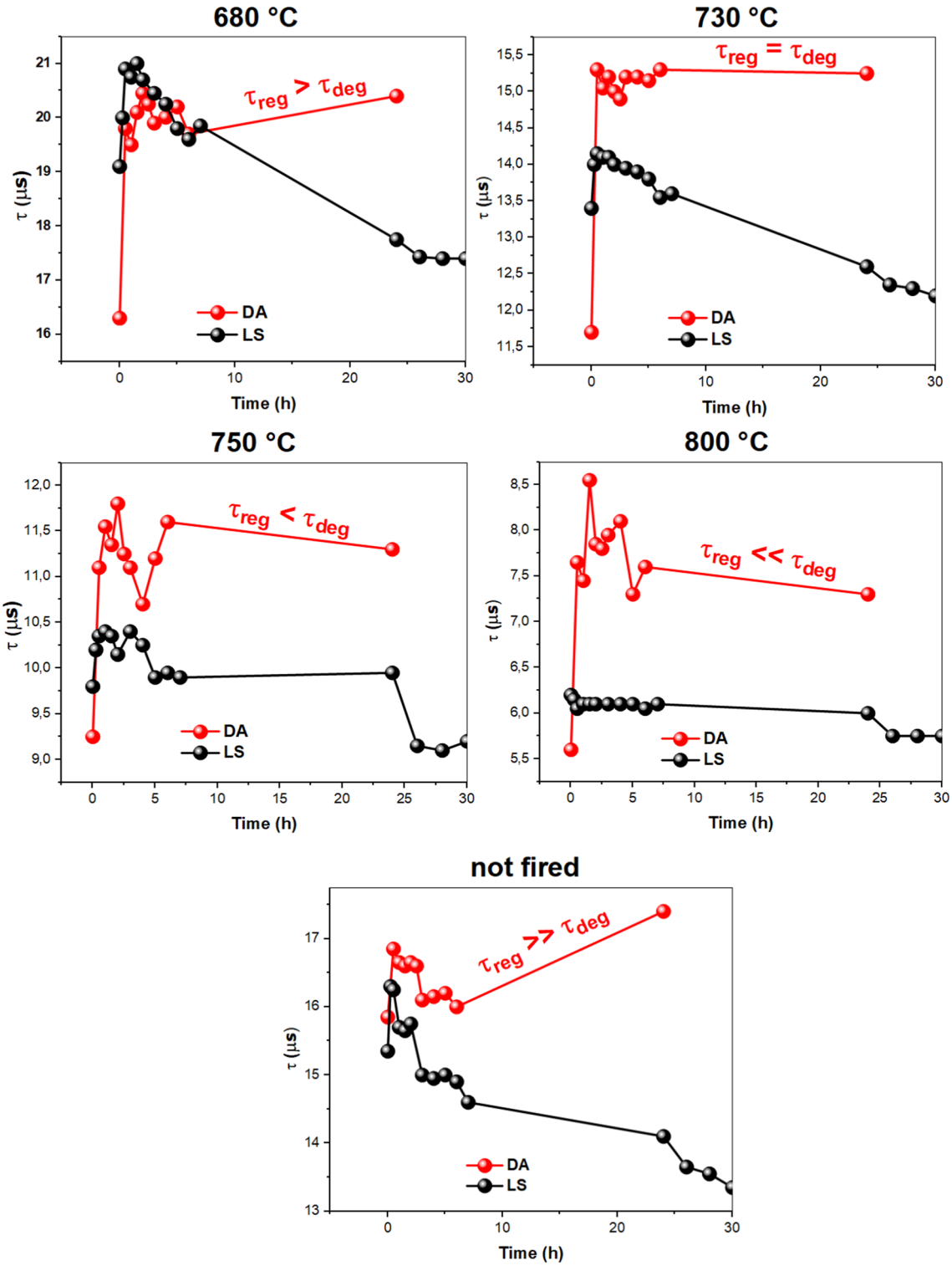

Fig. 6 Minority carrier lifetime as a function of time for: DA test (red color) at 160 °C and LS test (black color) at 35 °C of fired (from 680 to 800 °C) and unfired wafers for a duration of 30 h

[59–62]. It seems there is a consensus on the involvement of hydrogen in this degradation [59, 63–67]. This theory introduces "hydrogen-induced recombination" (HIR) [68], hydrogen displays amphoteric behavior in various semiconductors, including silicon, where it can be found in both positive (H^+) and negative states (H^-) [3, 13, 69]. It is an acceptor and a donor in n-type and p-type Si, respectively [12]. The fractional populations of free H charge states as a function of temperature have been described by Sun et al. [70].

As a consequence of the fast cool-down ramp and rapidly decreasing solubility, atomic hydrogen predominantly forms dimers, whereby it also already comes to some extent to the formation of dopant-hydrogen pairs [71]. The Hydrogen atoms then tend to associate with dopants, resulting in the formation of new complex such as H–B complexes [22, 69, 72–74]. The dopant, which is boron, would have acted as a catalyst for the breaking of hydrogen dimers and facilitated the formation of B–H pairs [75, 76]. The firing step leads to the incorporation of hydrogen from the surface layer of hydrogen-rich nitride [77], the concentration of incorporated hydrogen can reach 3.10^{15} cm^{-3} [60]. The SiNx:H layer is generally used as a hydrogen source for silicon solar cells [13]. The released hydrogen fraction from the SiNx:H layer, as detected from the results of FTIR and PL measurements after firing, correlated with the degradation of the lifetime in DA test (Fig. 6).

3.4 Simulation of LID-related degradation posits two independent defect states

To elucidate the variation of fast and slow boron-oxygen atoms combination in the silicon wafers, main recombination active defects source of light induced degradation during the illumination test and known as BO-LID [5, 15, 26–28, 34]. A kinetic model was developed employing Python code using ordinary differential equation (ODE) [39]. This model is based on two distinct BO defect theories [34]. Figure 7 represent the BO-LID kinetic model based on the two-defect theory.

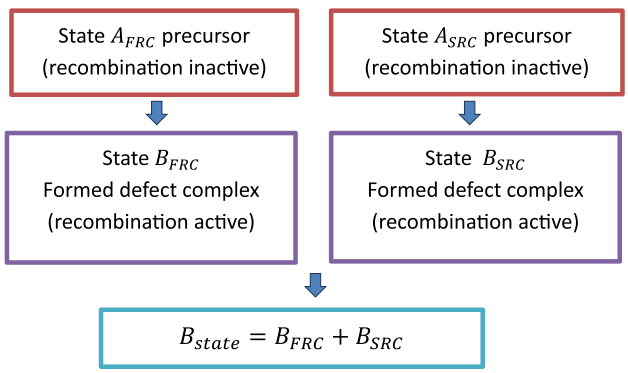

Fig. 7 State diagram and the transitions that are involved in BO defects based on the two-defect theory

The two-defect theory posits the existence of two independent precursor states A_{FRC} and A_{SRC} for fast recombination (FRC) and slow recombination (SRC) centers, respectively, along with two corresponding independent defect states B_{FRC} and B_{SRC}. The defect concentration in each state is denoted by $N_{i,}$ where i represents the specific state A_{FRC}, A_{SRC}, B_{FRC}, or B_{SRC}. The time evolution of each species concentration is governed by a system of linear differential equations.

$$\frac{dN_{A_{FRC}}}{dt} = -k_{AB_{FRC}}.N_{A_{FRC}} + k_{BA_{FRC}}.N_{B_{FRC}} + k_{FeB}.N_{FeB} \quad (1)$$

$$\frac{dN_{A_{SRC}}}{dt} = -k_{AB_{SRC}}.N_{A_{SRC}} + k_{BA_{SRC}}.N_{B_{SRC}} + k_{FeB}.N_{FeB} \quad (2)$$

$$\frac{dN_{B_{FRC}}}{dt} = -\frac{dN_{A_{FRC}}}{dt} \quad (3)$$

$$\frac{dN_{B_{SRC}}}{dt} = -\frac{dN_{A_{SRC}}}{dt} \quad (4)$$

The model further incorporates the influence of iron–boron (Fe–B) complex dissociation on the degradation process and the generation of new free boron atoms. This dissociation [78] is represented by the following chemical equation:

$$FeB + h^+ \rightarrow Fe + B \quad (5)$$

The rate of change in Fe-B concentration is described by:

$$\frac{dN_{FeB}}{dt} = -k_{FeB}.N_{FeB} \quad (6)$$

where, $N_{A_{FRC}}$: concentration of the A_{FRC} precursor. $N_{A_{SRC}}$: concentration of the A_{SRC} precursor. $N_{B_{FRC}}$: concentration of the B_{FRC} defect. $N_{B_{SRC}}$: concentration of the B_{SRC} defect. N_{FeB}: concentration of the Fe-B complex. $k_{AB_{FRC}}$: rate constant for the transition from precursor A_{FRC} to defect B_{FRC}. $k_{AB_{SRC}}$: rate constant for the transition from precursor A_{SRC} to defect B_{SRC}. $k_{BA_{FRC}}$: rate constant for the transition from defect B_{FRC} to precursor A_{FRC}. $k_{BA_{SRC}}$: rate constant for the transition from defect B_{SRC} to precursor A_{SRC}. k_{FeB}: rate constant for FeB dissociation.

The first two equations (Eqs. 1 and 2) depict the rate of change in the concentrations of FRC and SRC precursor states A. Equations three and four (Eqs. 3 and 4) represent conservation equations, ensuring the constant total concentration of both FRC and SRC defect states B. Finally, the

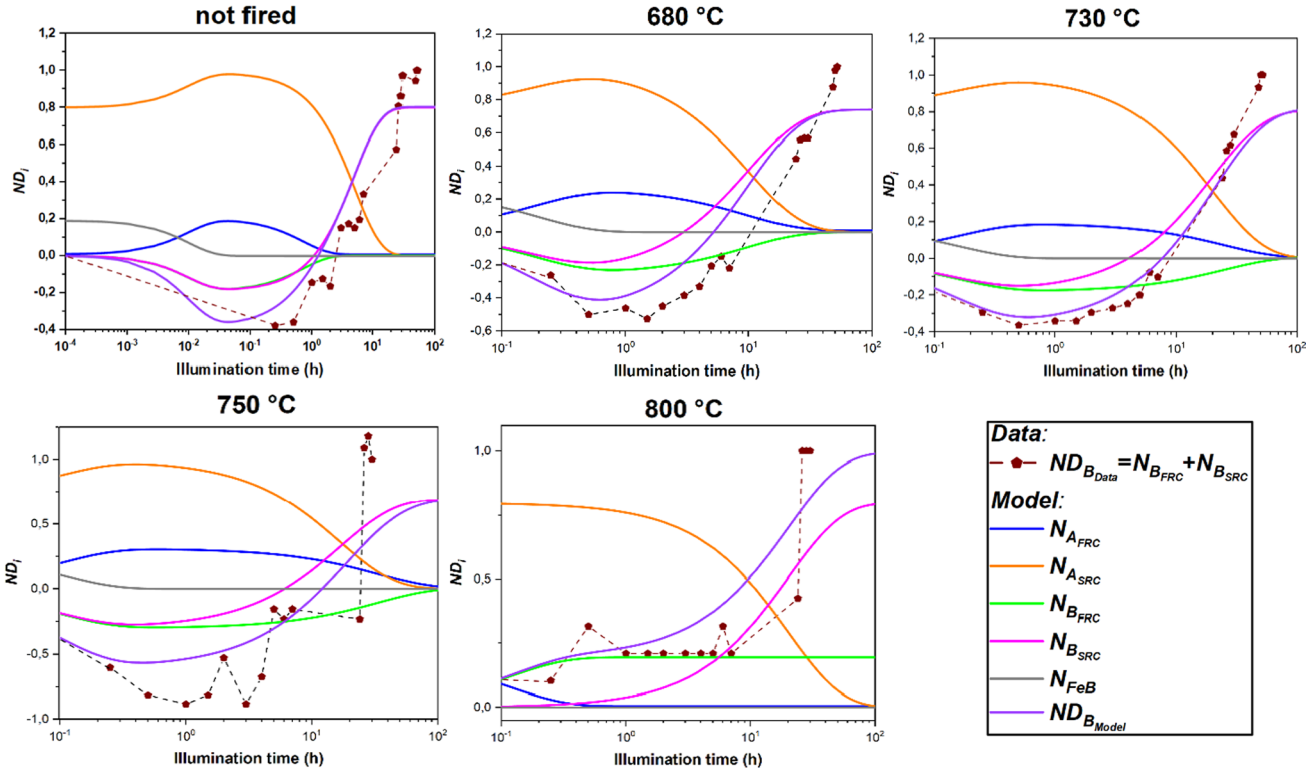

Fig. 8 Normalized concentration of different states $ND_i = \left(N_i/N_{dop}\right)$ as a function of time using reaction rate constants, experimental and simulated based on two defects theory

sixth equation (Eq. 6) describes the rate of change in Fe–B complex concentration.

The expected concentrations in the different states as a function of time for the two-defect theory are shown in Fig. 8. There is a clearly trends between the normalized concentration of defects in both simulated and experimental results as a function of illumination time. The two-stage degradation theory can adequately explain the evolution of carrier lifetime under illumination conditions.

To investigate the effect of temperature on defect generation, the experimental (Data) and simulated (Model) results were plotted to visualize the evolution of the normalized defect concentration ND_B with increasing Rapid Thermal Processing (RTP) peak temperature (Fig. 9a). In addition, the mean square error (MSE) method was selected (Fig. 9b) to capture the data vs. model error associated with the specific RTP peak temperature. As can be seen in Fig. 9a, the simulation shows a direct correlation between RTP peak temperature and ND_B. The model also predicts a progressive increase in the total defect population as the RTP temperature increases.

In this section, we present a comprehensive analysis of the rate constants related to the formation of various defects associated with the boron– oxygen interaction in silicon wafers. The Fig. 10 illustrates the temperature-dependent trends for the rate constants, specifically those associated with the fast defect $\left(k_{AB_{FRC}}\right)$, the slow defect $\left(k_{AB_{SRC}}\right)$, and the dissociation rate of the Fe-B complex $\left(k_{FeB}\right)$. The simulation indicates a significant correlation between the behavior of $k_{AB_{FRC}}$ and k_{FeB}, both of which exhibit a rapid decrease to a minimum value at the temperature peak of 680 °C within the RTP process. The kinetic reactions demonstrate an upward trend, following the increase in the peak temperature during the RTP process. Kim et al. [79] point out that the apparently higher k_{FRC} of the FRC degradation may be a consequence of the combination of Fe and B-O defects, which is in good agreement with our model results. In contrast, the rate constant responsible for slow defect formation $k_{AB_{SRC}}$, appears to be independent of the release of the free boron atoms resulting from the dissociation of Fe-B complexes. Moreover, $k_{AB_{SRC}}$ decreases with increasing peak temperatures during the RTP process. One potential explanation is the presence of hydrogen in the SiNx:H layer, which can passivate the volume of the silicon wafers after the RTP process by diffusion [13, 14, 22, 60, 77, 80, 82–84] and association with boron atoms [29, 69, 71–76, 85, 86]. In addition, the results suggest that the behavior of FRC is related by the concentration of free boron atoms that result from the

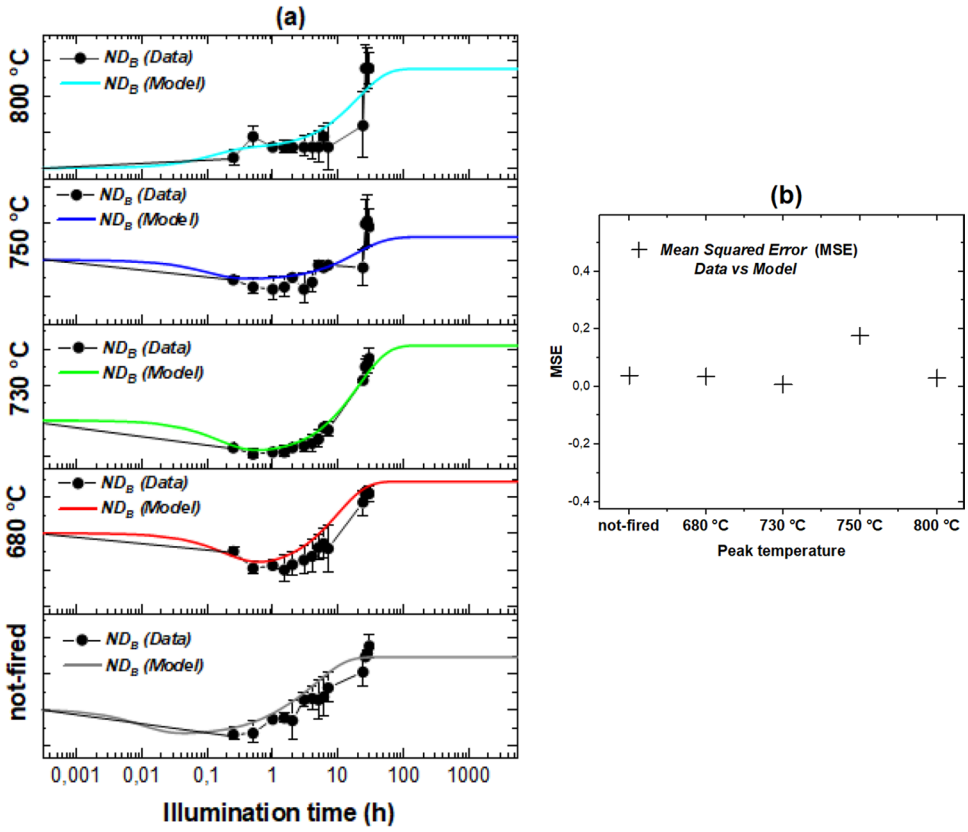

Fig. 9 Shows **a** the normalized concentration of defect ND_B: experimental (data) and simulation (model) as function of illumination time. **b** The mean squared error (MSE) between the data and model

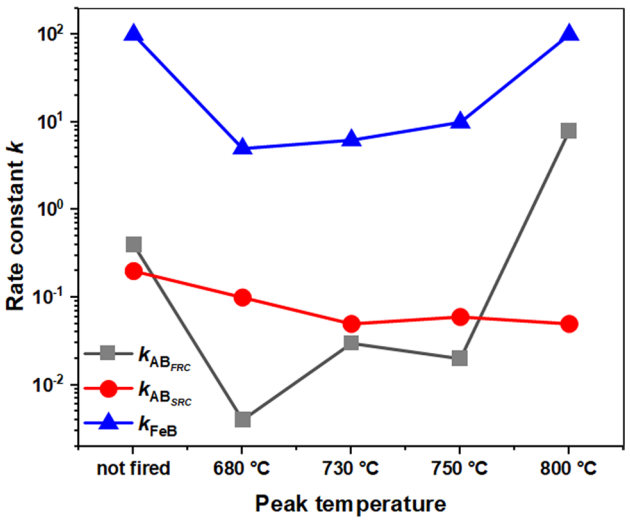

Fig. 10 The rate constants of formation of the fast defect $k_{AB_{FRC}}$, the slow defect $k_{AB_{SRC}}$ and the dissociation of the Iron-Boron complex k_{FeB} as a function of peak temperature

breaking bonds of Fe-B pears. The B_{FRC} defects competes directly with the charge released from of FeB dissociation, which leads to a regeneration in carrier lifetime during the initial illumination phase of the light-induced degradation (LID) test. This phenomenon was observed in simulations of different species (see Fig. 9), where the defect concentration of the B_{FRC} state is exceeded by the charge released by Fe-B dissociation. However, silicon wafers undergoing high-temperature RTP processes (800 °C) do not demonstrate a similar rise in carrier lifetime during the initial phase of the LS test, in contrast to other samples. The possible rise of new thermally defects [87, 88] and degradation of the SiNx:H passivation layer [88] for samples treated at elevated temperatures 800 °C, can be responsible for this disparity. It is worth noting that the duration of light exposure in the LS test does not affect these thermally induced defects. Therefore, these thermally defects effectively capture excess charges resulting from the dissociation of Fe–B complexes, promoting the dominance of the FRC state in the earlier stage of illumination, as showed by the rapid increase in the rate constants for $k_{AB_{FRC}}$ at peaks 800 °C (see Fig. 10).

4 Conclusion

This study explored the parameters that affect minority carrier lifetime in boron-doped silicon wafers passivated with SiNx:H layers. Experimental techniques such as QSSPC, FTIR, and PL spectroscopy were employed alongside simulation based on the two-defect theory to demonstrate how temperature, defect formation, and illumination jointly

influence the behavior of the carrier lifetime. The dynamics of Fe–B dissociation rate significantly impacted the earlier stage of the illumination process, while the slower defect formation rate appears to be independent of this factor. However, it decreases at higher RTP temperatures, possibly due to hydrogen diffusion and association with boron atoms. Furthermore, distinct lifetime values revealed by DA compared to LS tests led to the concept of hydrogen-induced recombination. Finally, these findings provide evidence of various influential factors impacting stability of τ offering novel insights into silicon semiconductor materials, thereby contributing towards enhancing reliability and efficiency stability for Si-based solar cells under operational conditions.

Acknowledgements The authors express their gratitude to the characterization staff service of the Research Center in Semiconductor Technology for Energy (CRTSE) Algiers and the Department of Physics, Faculty of Science, University of Badji Mokhtar Annaba, Algeria, for their invaluable support. This work received funding from the General Direction of Scientific Research and Technological Development of Algeria (DGRSDT/MESRS).

Author contributions Study conception and design: Y. Chibane, Y. Kouhlane. Data collection: Y. Chibane, D. Bouhafs. Analysis of results: Z. W. Achour, A. Mohammed-Krarroubi, A. Khelfane. Interpretation of results: Y. Chibane, Y. Kouhlane. Draft manuscript preparation: Y. Chibane, Y. Kouhlane, D. Bouhafs. All authors reviewed the results and approved the final version of the manuscript.

Data availability The data underlying this study are available in the published article.

Declarations

Conflict of interest All authors declare that they have no conflicts of interest.

References

1. ITRPV, International Technology Roadmap for Photovoltaic (ITRPV), (10th ed) 2019, pp. 1–38. https://pv-manufacturing.org/wp-content/uploads/2019/03/ITRPV-2019.pdf
2. M. Green, What's next in photovoltaics beyond PERC? In: APSRC, 2018, 'Proceedings of the Asia Pacific Solar Research Conference 2018', Publisher: Australian PV Institute, 2018, ISBN: 978-0-6480414-2-9. https://apvi.org.au/solar-research-conference/proceedings-apsrc-2018/
3. D. Chen, Elucidating the mechanics behind light- and elevated temperature-induced degradation in silicon solar cells. Thesis, UNSW, Sydney, (2020) https://doi.org/10.13140/RG.2.2.10653.33762
4. Y. Zhongshu, J. Krügener, F. Feldmann, J.-I. Polzin, B. Steinhauser, T. Le, D. Macdonald, A. Liu, Impurity gettering in polycrystalline-silicon based passivating contacts—the role of oxide stoichiometry and pinholes. Adv. Energy Mater. **12**, 2103773 (2022). https://doi.org/10.1002/aenm.202103773
5. L.I. Khirunenko, M.G. Sosnin, A.V. Duvanskii, N.V. Abrosimov, H. Riemann, New properties of boron–oxygen dimer defect in boron-doped Czochralski silicon. J. Appl. Phys. **132**(13), 135703 (2022). https://doi.org/10.1063/5.0114809
6. ITRPV, International Technology Roadmap for Photovoltaic (ITRPV), 2022 Results, 14th ed. (VDMA 2023). https://www.vdma.org/international-technology-roadmap-photovoltaic
7. Photovoltaics Report, Fraunhofer Institute for Solar Energy Systems ISE: Fraunhofer Institute for Solar Energy Systems ISE, (2020). https://fr.scribd.com/document/641697041/Photovoltaics-Report-Fraunhofer-2020.
8. A. Shahzad, S. Khatun, S. Sallam, A. Ansari, Z.A. Ansari, R.R. Kumar, J. Hakami, A. Khan, Photoresponse of porous silicon for potential optical sensing. Europhys. Lett. **139**(3), 36001 (2022). https://doi.org/10.1209/0295-5075/ac7d08
9. A. Shahzad, A. Ansari, M.A. Siddiqui, A. Khan, P. Ranjan, A potential optical sensor based on nanostructured silicon. J. Mater. Sci. Mater. Electron. **34**(8), 755 (2023). https://doi.org/10.1007/s10854-023-10187-2µ
10. W.K. Hamoudi, R.A. Ismail, K. Al-Qayim, D.N. Raouf, R.H. Mahdi, M.S. Murad, Effect of rapid thermal annealing on photovoltaic properties of silicon solar cell fabricated by one-step laser doping in liquid. Appl. Phys. A **130**(1), 26 (2023). https://doi.org/10.1007/s00339-023-07173-0
11. M.S. Prasanna, P. Kale, State-of-the-art passivation strategies of c-Si for photovoltaic applications: a review. Mater. Sci. Semicond. Process. **154**, 107202 (2023). https://doi.org/10.1016/j.mssp.2022.107202
12. J. Coutinho, G. Diana, V.J.B. Torres, T.O. Abdul Fattah, V.P. Markevich, A.R. Peaker, Hydrogen reactions with dopants and impurities in solar silicon from first principles. Solar RRL (2023). https://doi.org/10.1002/solr.202300639
13. L. Song, Z. Hu, D. Lin, D. Yang, X. Yu, Progress of hydrogenation engineering in crystalline silicon solar cells: a review. J. Phys. D Appl. Phys. (2022). https://doi.org/10.1088/1361-6463/ac9066/meta
14. A. Liu, S. Pheng-Phang, D. Macdonald, Gettering in silicon photovoltaics: a review. Solar Energy Mater. Solar Cells **234**, 111447 (2022). https://doi.org/10.1016/j.solmat.2021.111447
15. J. Schmidt, K. Bothe, Performance-limiting oxygen-related defects in silicon solar cells. ECS Trans. **3**(4), 285 (2006). https://doi.org/10.1149/1.2355764
16. C. Sen, C. Chan, P. Hamer, M. Wright, C. Chong, B. Hallam, M. Abbott, «Eliminating light- and elevated temperature-induced degradation in P-type PERC solar cells by a two-step thermal process. Sol. Energy Mater. Sol. Cells **209**, 110470 (2020). https://doi.org/10.1016/j.solmat.2020.110470
17. K. Kim, R. Chen, D. Chen, P. Hamer, A. Ciesla-Nee-Wenham, S. Wenham, Z. Hameiri, Degradation of surface passivation and bulk in p-type monocrystalline silicon wafers at elevated temperature. IEEE J. Photovolt. **9**, 97–105 (2019). https://doi.org/10.1109/JPHOTOV.2018.2878791
18. X. Tan, Insights into the mechanisms of bulk and surface related degradation in monocrystalline silicon solar cells. Thesis, UNSW Sydney, (2020). https://doi.org/10.26190/unsworks/22239.
19. T. O. Abdul Fattah, J. Jacobs, V. P. Markevich, N. V. Abrosimov, M. P. Halsall, I. F. Crowe, A. R. Peaker, Analysis of impurity-related radiative transitions in silicon materials using temperature-dependent photoluminescence. In: 2023 IEEE 50th Photovoltaic Specialists Conference (PVSC), 1–6 (2023). https://doi.org/10.1109/PVSC48320.2023.10359855
20. C. Sen, P. Hamer, A. Soeriyadi, B. Wright, M. Wright, A. Samadi, D. Chen, B.V. Stefani, D. Zhang, J. Wu, F. Jiang, B. Hallam, M. Abbott, Impact of surface doping profile and passivation layers on surface-related degradation in silicon PERC solar cells. Sol. Energy Mater. Sol. Cells **235**, 111497 (2022). https://doi.org/10.1016/j.solmat.2021.111497

21. S. Yuan, S. Ding, B. Ai, D. Chen, J. Jin, J. Ye, D. Qiu, X. Sun, X. Liang, In situ LID and regeneration of PERC solar cells from different positions of a B-doped Cz-Si ingot. Int. J. Photoenergy **2022**, 6643133 (2022). https://doi.org/10.1155/2022/6643133
22. D. Lin, Z. Hu, Q. He, D. Yang, L. Song, X. Yu, New insights on LeTID/BO-LID in p-type mono-crystalline silicon. Sol. Energy Mater. Sol. Cells **226**, 111085 (2021). https://doi.org/10.1016/j.solmat.2021.111085
23. S. Ding, C. Yang, C. Qin, B. Ai, X. Sun, J. Yang, Q. Liu, X. Liang, Comparison of LID and electrical injection regeneration of PERC and Al-BSF solar cells from a Cz-Si ingot. Energies **15**, 7764 (2022). https://doi.org/10.3390/en15207764
24. B. Hammann, N. Assmann, P. Weiser, W. Kwapil, T. Niewelt, F. Schindler, R. Søndenå, E.V. Monakhov, M. Schubert, The impact of different hydrogen configurations on light- and elevated-temperature-induced degradation. IEEE J. Photovolt. (2023). https://doi.org/10.1109/JPHOTOV.2023.3236185
25. M. H. Utila, C-H Lin, LeTID study of passivation layers for Si solar cells. In: Advanced Photonics Congress 2023 (2023), Paper SW3D.4, SW3D.4. Optica Publishing Group, (2023). https://doi.org/10.1364/SELED.2023.SW3D.4
26. M. Kim, M. Abbott, N. Nampalli, S. Wenham, B. Stefani, B. Hallam, Modulating the extent of fast and slow boron-oxygen related degradation in Czochralski silicon by thermal annealing: evidence of a single defect. J. Appl. Phys. **121**(5), 053106 (2017). https://doi.org/10.1063/1.4975685
27. T. Niewelt, J. Schön, W. Warta, S.W. Glunz, M.C. Schubert, Degradation of crystalline silicon due to boron–oxygen defects. IEEE J. Photovolt. **7**(1), 383–398 (2016). https://doi.org/10.1109/JPHOTOV.2016.2614119
28. J. Lindroos, H. Savin, Review of light-induced degradation in crystalline silicon solar cells. Sol. Energy Mater. Sol. Cells **147**, 115–126 (2016). https://doi.org/10.1016/j.solmat.2015.11.047
29. B.J. Hallam, P.G. Hamer, S. Wang, L. Song, N. Nampalli, M.D. Abbott, C.E. Chan, D. Lu, A.M. Wenham, L. Mai, N. Borojevic, A. Li, D. Chen, M.Y. Kim, A. Azmi, S. Wenham, Advanced hydrogenation of dislocation clusters and boron–oxygen defects in silicon solar cells. Energy Procedia. **77**, 799–809 (2015). https://doi.org/10.1016/j.egypro.2015.07.113
30. J. Lindroos, Copper-related light-induced degradation in crystalline silicon. Thesis, Aalto University, Finland, (2015). https://urn.fi/URN:ISBN:978-952-60-6130-6
31. A. Salam, R. Ismail, M.A. Mohammed, HgI2@CsI core/shell nanoparticles: synthesis, characterization, and application in photosensors. J. Indian Chem. Soc. **99**(7), 100515 (2022). https://doi.org/10.1016/j.jics.2022.100515
32. A. Mohammed-Krarroubi, Effect of gettering on the degradation/regeneration mechanisms induced by charge carrier injection on the performance of p-type silicon-based solar cells. Confirmation report, Semiconductor Technology Research Center for Energy (CRTSE), ALGIERS, (2021)
33. R.A. Sinton, A. Cuevas, Contactless determination of current–voltage characteristics and minority-carrier lifetimes in semiconductors from quasi-steady-state photoconductance data. Appl. Phys. Lett. **69**(17), 2510–2512 (1996). https://doi.org/10.1063/1.117723
34. K. Bothe, J. Schmidt, Electronically activated boron–oxygen-related recombination centers in crystalline silicon. J. Appl. Phys. **99**, 013701 (2006). https://doi.org/10.1063/1.2140584
35. A.A. Istratov, H. Hieslmair, E.R. Weber, Iron and its complexes in silicon. Appl. Phys. A Mater. Sci. Process. **69**, 13–44 (1999). https://doi.org/10.1007/s003390050968
36. J.H. Reiss, R.R. King, K.W. Mitchell, Characterization of diffusion length degradation in Czochralski silicon solar cells. Appl. Phys. Lett. **68**, 3302–3304 (1996). https://doi.org/10.1063/1.116581
37. X. Zhu, D. Yang, X. Yu, J. He, Y. Wu, J. Vanhellemont, D. Que, Iron-boron pair dissociation in silicon under strong illumination. AIP Adv. **3**, 082124 (2013). https://doi.org/10.1063/1.4819481
38. C. Möller, T. Bartel, F. Gibaja, K. Lauer, Iron–boron pairing kinetics in illuminated p-type and in boron/phosphorus co-doped n-type silicon. J. Appl. Phys. **116**, 024503 (2014). https://doi.org/10.1063/1.4889817
39. M. Kim, Understanding the mechanisms of light-induced degradation in crystalline silicon. Thesis, UNSW, Sydney, (2020). https://doi.org/10.26190/unsworks/22278
40. D. Macdonald, T. Roth, P.N.K. Deenapanray, T. Trupke, R.A. Bardos, Doping dependence of the carrier lifetime crossover point upon dissociation of iron–boron pairs in crystalline silicon. Appl. Phys. Lett. **89**, 142107 (2006). https://doi.org/10.1063/1.2358126
41. O. Olikh, V. Kostylyov, V. Vlasiuk, R. Korkishko, R. Chupryna, intensification of iron–boron complex association in silicon solar cells under acoustic wave action. J. Mater. Sci. Mater. Electron. **33**(16), 13133–13142 (2022). https://doi.org/10.1007/s10854-022-08252-3
42. K. Kim, S.K. Dhungel, J. Yoo, S. Jung, D. Mangalaraj, J. Yi, Hydrogenated silicon-nitride thin films as antireflection and passivation coatings for multicrystalline silicon solar cells. J. Korean Phys. Soc. **51**(5), 1659–1662 (2007). https://doi.org/10.3938/jkps.51.1659
43. W.D. Brown, M.A. Khaliq, The effects of rapid thermal annealing on the properties of plasma-enhanced chemically vapor-deposited silicon nitride. Thin Solid Films **186**(1), 73–85 (1990). https://doi.org/10.1016/0040-6090(90)90501-4
44. Y. Liu, N. Jehanathan, J. Dell, Thermally induced damages of PECVD SiNx thin films. J. Mater. Res. **26**(19), 2552–2557 (2011). https://doi.org/10.1557/jmr.2011.236
45. B. Karunagaran, S.J. Chung, S. Velumani, E.-K. Suh, Effect of rapid thermal annealing on the properties of PECVD SiNx thin films. Mater. Chem. Phys. **106**(1), 130–133 (2007). https://doi.org/10.1016/j.matchemphys.2007.05.028
46. S. Rein, S.W. Glunz, Electronic properties of interstitial iron and iron–boron pairs determined by means of advanced lifetime spectroscopy. J. Appl. Phys. **98**, 113711 (2005). https://doi.org/10.1063/1.2106017
47. K. Lauer, C. Möller, D. Debbih, M. Auge, D. Schulze, Determination of activation energy of the iron acceptor pair association and dissociation reaction. Solid State Phenom. **242**, 230–235 (2015). https://doi.org/10.4028/www.scientific.net/SSP.242.230
48. D. Macdonald, T. Roth, P.N.K. Deenapanray, K. Bothe, P. Pohl, J. Schmidt, Formation rates of iron-acceptor pairs in crystalline silicon. J. Appl. Phys. **98**, 083509 (2005). https://doi.org/10.1063/1.2102071
49. E. Bustarret, M. Bensouda, M.C. Habrard, J.C. Bruyère, S. Poulin, S.C. Gujrathi, Configurational statistics in a-SixNyHz alloys: a quantitative bonding analysis. Phys. Rev. B Condens. Matter **38**(12), 8171–8184 (1998). https://doi.org/10.1103/physrevb.38.8171
50. G. Scardera, T. Puzzer, G. Conibeer, M.A. Green, Fourier transform infrared spectroscopy of annealed silicon-rich silicon nitride thin films. J. App. Phy. **104**(10), 104310 (2008). https://doi.org/10.1063/1.3021158
51. S. Preet-Singh, G. Vijaya-Prakash, S. Ghosh, S. Rai, P. Srivastava, Impact of thermal annealing on interfacial layer and electrical properties of a-SiNx: H/Si. Euro Phys. Lett. (2010). https://doi.org/10.1209/0295-5075/90/26002
52. H.T. Nguyen, F.E. Rougieux, D. Yan, Y. Wan, S. Mokkapati, S.M. De Nicolas, J.P. Seif, S. De Wolf, D. Macdonald, Characterizing amorphous silicon, silicon nitride, and diffused layers in crystalline silicon solar cells using micro-photoluminescence

spectroscopy. Sol. Energy Mater. Sol. Cells **145**, 403–411 (2016). https://doi.org/10.1016/j.solmat.2015.11.006
53. R. Basnet, M. Siriwardhana, H. Nguyen, D. Macdonald, Impact of gettering and hydrogenation on sub-band-gap luminescence from ring defects in Czochralski-grown silicon. ACS Appl. Energy Mater. (2021). https://doi.org/10.1021/acsaem.1c02100
54. M.W. Lamers, K. Butler, I.G. Romijn, J. Harding, A.W. Weeber, Examination of the properties of the interface of a-SiNx:H/Si in crystalline silicon solar cells and its effect on cell efficiency. MRS Online Proc. Lib. **1423**, 7–12 (2012). https://doi.org/10.1557/opl.2012.56
55. F. Kersten, J. Heitmann, J.W. Müller, Influence of Al2O3 and SiNx passivation layers on LeTID. Energy Procedia **92**, 828–832 (2016). https://doi.org/10.1016/j.egypro.2016.07.079
56. D. Lin, Z. Hu, L. Song, D. Yang, X. Yu, Investigation on the light and elevated temperature induced degradation of gallium-doped Cz-Si. Sol. Energy **225**, 407–411 (2021). https://doi.org/10.1016/j.solener.2021.07.023
57. W. Kwapil, J. Dalke, R. Post, T. Niewelt, Influence of dopant elements on degradation phenomena in B- and Ga-doped Czochralski-Grown silicon. Solar RRL **5**(5), 2100147 (2021). https://doi.org/10.1002/solr.202100147
58. A. C. N. Wenham, S. Wenham, R. Chen, C. Chan, D. Chen, B. Hallam, D. Payne, T. Fung, M. Kim, S. Liu, S. Wang, K. Kim, A. Samadi, C. Sen, C. Vargas, U. Varshney, B. V. Stefani, P. Hamer, G. Bourret-Sicotte, N. Nampalli, Z. Hameiri, C. Chong, M. Abbott, Hydrogen-induced degradation. In: 2018 IEEE 7th World Conference on Photovoltaic Energy Conversion, WCPEC 2018—a joint conference of 45th IEEE PVSC, 28th PVSEC and 34th EU PVSEC 2018, pp. 1–8. https://doi.org/10.1109/PVSC.2018.8548100
59. B. Hammann, L. Rachdi, W. Kwapil, F. Schindler, M.C. Schubert, Insights into the hydrogen-related mechanism behind defect formation during light- and elevated temperature-induced degradation. Phys. Status Solidi Rapid Res. Lett. **15**, 2000584 (2021). https://doi.org/10.1002/pssr.202000584
60. D.C. Walter, V.V. Voronkov, R. Falster, D. Bredemeier, J. Schmidt, On the kinetics of the exchange of hydrogen between hydrogen–boron pairs and hydrogen dimers in crystalline silicon. J. Appl. Phys. **131**, 165702 (2022). https://doi.org/10.1063/5.0086307
61. J. Simon, A. Herguth, G. Hahn, Quantitative analysis of boron–hydrogen pair dynamics by infrared absorption measurements at room temperature. J. Appl. Phys. **131**, 235703 (2022). https://doi.org/10.1063/5.0090965
62. V.V. Voronkov, Independent subsystems of atomic hydrogen in silicon responsible for boron passivation and for dimer production. Phys. Status Solidi A **219**, 2200081 (2022). https://doi.org/10.1002/pssa.202200081
63. D. Chen, P.G. Hamer, M. Kim, T.H. Fung, G. Bourret-Sicotte, S. Liu, C.E. Chan, A. Ciesla, R. Chen, M.D. Abbott, B.J. Hallam, S.R. Wenham, Hydrogen induced degradation: a possible mechanism for light- and elevated temperature- induced degradation in n-type silicon. Sol. Energy Mater. Sol. Cell. **185**, 174–182 (2018). https://doi.org/10.1016/j.solmat.2018.05.034
64. D. Chen, M. Vaqueiro Contreras, A. Ciesla, P. Hamer, B. Hallam, M. Abbott, C. Chan, Progress in the understanding of light- and elevated temperature-induced degradation in silicon solar cells: a review. Prog. Photovolt. Res. Appl. **29**, 1180–1201 (2020). https://doi.org/10.1002/pip.3362
65. T. Niewelt, F. Schindler, W. Kwapil, R. Eberle, J. Schon, M.C. Schubert, Understanding the light-induced degradation at elevated temperatures: similarities between multicrystalline and float-zone p-type silicon. Prog. Photovolt. Res. Appl. **26**, 533–542 (2018). https://doi.org/10.1002/pip.2954
66. M. Winter, D. Walter, J. Schmidt, Carrier lifetime degradation and regeneration in gallium- and boron-doped monocrystalline silicon materials. IEEE J. Photovolt. **11**, 866–872 (2021). https://doi.org/10.1109/jphotov.2021.3070474
67. D. Bredemeier, D.C. Walter, R. Heller, J. Schmidt, Impact of hydrogen-rich silicon nitride material properties on light-induced lifetime degradation in multicrystalline silicon. Phys. Status Solidi Rapid Res. Lett. **13**, 1900201 (2019). https://doi.org/10.1002/pssr.201900201
68. C. Herring, N.M. Johnson, C.G. Van de Walle, Energy levels of isolated interstitial hydrogen in silicon. Phys. Rev. B **64**(12), 125209 (2001). https://doi.org/10.1103/PhysRevB.64.125209
69. Y. Acker, J. Simon, A. Herguth, Formation dynamics of BH and GaH-Pairs in crystalline silicon during dark annealing. Physica Status Solidi (a) **219**(17), 2200142 (2022). https://doi.org/10.1002/pssa.202200142
70. C. Sun, D. Yan, D. Macdonald, Modeling the charge state of monatomic hydrogen and other defects with arbitrary concentrations in crystalline silicon. Phys. Status Solidi (RRL)—Rapid Res. Lett. **15**, 2100483 (2021). https://doi.org/10.1002/pssr.202100483
71. C. Winter, J. Simon, A. Herguth, Study on boron–hydrogen pairs in bare and passivated float-zone silicon wafers. Physica Status Solidi (a) **218**(23), 2100220 (2021). https://doi.org/10.1002/pssa.202100220
72. C.G. Van de Walle, J. Neugebauer, Hydrogen in semiconductors. Ann. Rev. Mater. Res. **36**(1), 179–198 (2006). https://doi.org/10.1146/annurev.matsci.36.010705.155428
73. J. Simon, A. Herguth, L. Kutschera, G. Hahn, The dissociation of gallium–hydrogen pairs in crystalline silicon during illuminated annealing. Phys. Status Solidi Rapid Res. Lett. **16**, 2200297 (2022). https://doi.org/10.1002/pssr.202200297
74. D.C. Walter, D. Bredemeier, R. Falster, V.V. Voronkov, J. Schmidt, Easy-to-apply methodology to measure the hydrogen concentration in boron-doped crystalline silicon. Sol. Energy Mater. Sol. Cell. **200**, 109970 (2019). https://doi.org/10.1016/j.solmat.2019.109970
75. J. Coutinho, D. Gomes, V.J.B. Torres, T.O. Abdul Fattah, V.P. Markevich, A.R. Peaker, Theory of reactions between hydrogen and group-III acceptors in silicon. Phys. Rev. B **108**(1), 014111 (2023). https://doi.org/10.1103/PhysRevB.108.014111
76. D. Gomes, V.P. Markevich, A.R. Peaker, J. Coutinho, Dynamics of hydrogen in silicon at finite temperatures from first principles. Physica Status Solidi (b) **259**(6), 2100670 (2022). https://doi.org/10.1002/pssb.202100670
77. V.V. Voronkov, R. Falster, Generation and loss of hydrogen-boron pairs in fired silicon wafers. Mater. Sci. Semicond. Process. **167**, 107796 (2023). https://doi.org/10.1016/j.mssp.2023.107796
78. J.E. Birkholz, K. Bothe, D. Macdonald, J. Schmidt, Electronic properties of iron-boron pairs in crystalline silicon by temperature -and injection-level-dependent lifetime measurements. J. Appl. Phys. **97**, 103708 (2005). https://doi.org/10.1063/1.1897489
79. M. Kim, D. Chen, M. Abbott, N. Nampalli, S. Wenham, B. Stefani, B. Hallam, Impact of interstitial iron on the study of metastable BO defects in Czochralski silicon: Further evidence of a single defect. J. Appl. Phys. **123**, 16 (2018)
80. Y. Kouhlane, D. Bouhafs, N. Khelifati, A. Guenda, N.E. Demagh, A. Demagh, P. Pfeiffer, S. Mezghiche, W. Hetatache, F. Derkaoui, C. Nasraoui, O.V. Nwadiaru, Thermal stress during RTP processes and its possible effect on the light induced degradation in Cz-Si wafers. Heat Mass Transf. **54**, 3081–3087 (2018). https://doi.org/10.1007/s00231-018-2355-x
81. B.J. Hallam, C.E. Chan, R. Chen, S. Wang, J. Ji, L. Mai, D.M. Abbott, D.N. Payne, M. Kim, D. Chen, C. Chong, S.R. Wenham, Rapid mitigation of carrier-induced degradation in commercial silicon solar cells. Jpn. J. Appl. Phys. (2017). https://doi.org/10.7567/JJAP.56.08MB13

82. Y. Kouhlane, D. Bouhafs, A. Guenda, N. Demagh, A. Guessoum, A. Chibani, RTP process effect on multicrystalline mc-Si wafers and its impact on solar cell efficiency. In: Conference: 47th IEEE Photovoltaic Specialists Conference (PVSC)At: virtual meeting, Volume: 47, Calgary, AB, Canada, https://doi.org/10.1109/PVSC45281.2020.9301013
83. L. Helmich, D.C. Walter, D. Bredemeier, J. Schmidt, Atomic-layer deposited Al2O3 as effective barrier against the diffusion of hydrogen from SiNx:H layers into crystalline silicon during rapid thermal annealing. Phys. Status Solidi Rapid Res. Lett. **14**(12), 2000367 (2020). https://doi.org/10.1002/pssr.202000367
84. D. Bredemeier, D.C. Walter, J. Schmidt, Lifetime degradation in multicrystalline silicon under illumination at elevated temperatures: indications for the involvement of hydrogen. Proc. Amer. Inst. Phys. Conf. (2018). https://doi.org/10.1063/1.5049320
85. N. Nampalli, B. Hallam, C. Chan, M. Abbott, S. Wenham, Evidence for the role of hydrogen in the stabilization of minority carrier lifetime in boron-doped Czochralski silicon. Appl. Phys. Lett. **106**, 173501 (2015). https://doi.org/10.1063/1.4919385
86. S. Wilking, C. Beckh, S. Ebert, A. Herguth, G. Hahn, Influence of bound hydrogen states on BO-regeneration kinetics and consequences for high-speed regeneration processes. Sol. Energy Mater. Sol. Cells **131**, 2–8 (2014). https://doi.org/10.1016/j.solmat.2014.06.027
87. J.Y. Lee, Rapid thermal processing in solar cells- passivation, and diffusion. Thesis, Freiburg (2003). https://www.freidok.uni-freiburg.de/dnb/download/1118
88. A. Castaldini, D. Cavalcoli, A. Cavallini, D. Jones, V. Palermo, E. Susi, Surface modifications in Si after rapid thermal annealing. J. Electrochem. Soc. **149**(12), G633 (2002). https://doi.org/10.1149/1.1516225